BIOCHEMISTRY
including biophysical chemistry & molecular biology

Article

pubs.acs.org/biochemistry

Ethylene Glycol Quenching of Nitrogenase Catalysis: An Electron Paramagnetic Resonance Spectroscopic Study of Nitrogenase Turnover States and CO Bonding

Brian J. Hales*

Department of Chemistry, Louisiana State University, Baton Rouge, Louisiana 70808, United States

Supporting Information

ABSTRACT: Most hydrophilic organic solvents inhibit enzymatic activity. Nitrogenase is shown to be approximately 3 times more sensitive to organic inhibition than most other soluble enzymes. Ethylene glycol (EG) is demonstrated to rapidly inhibit nitrogenase activity without uncoupling ATP hydrolysis. Our data suggest the mechanism of inhibition is EG's blocking of binding of MgATP to the nitrogenase Fe protein. EG quenching allows, for the first time, the observation of the relaxation of the intermediate reaction states at room temperature. Electron paramagnetic resonance (EPR) spectroscopy is used to monitor the room-temperature decay of the nitrogenase turnover states following EG quenching of catalytic activity. The return of the intermediate states to the resting state occurs in multiple phases over 2 h. During the initial stage, nitrogenase still possesses the ability to generate CO-induced EPR signals even though catalytic activity has ceased. During the last phase of relaxation, the one-electron reduced state of the MoFe protein ($\mathbf{E_1}$) relaxes to the resting state ($\mathbf{E_0}$) in a slow first-order reaction.

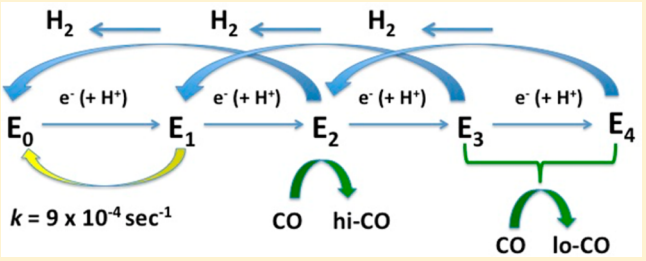

Nitrogenase, the enzyme responsible for the bioconversion of dinitrogen into ammonia, is a two-protein system.[1] One protein of Mo-nitrogenase (called the MoFe protein, component 1, or Av1 when isolated from *Azotobacter vinelandii*) is an $\alpha_2\beta_2$ tetramer containing two pairs of large metal clusters, the [Fe_8S_7] P-cluster and the [$MoFe_7S_9C$-homocitrate] FeMo cofactor or FeMoco. FeMoco is the site of substrate binding and reduction. (Another enzyme form, V-nitrogenase, has an analogous protein called the VFe protein that contains a FeV cofactor.)[2,3] The second protein of the enzyme, the Fe protein, component 2, or Av2, is a γ_2 dimer containing a single [Fe_4S_4] cluster and two MgATP binding sites.

In the native or resting state, FeMoco (M^N) in Av1 is EPR active ($S = {}^3/_2$ and g factors of 4.3, 3.6, and 2.0), while the P-cluster (P^N) is diamagnetic.[4] The resting state of Av2 ($Av2^{Rd}$) is also paramagnetic ($[Fe_4S_4]^+$), exhibiting an $S = {}^1/_2, {}^3/_2$ mixed spin state.[5] The first step of enzymatic turnover involves $Av2^{Rd}(MgATP)_2$ donating an electron to Av1 reducing FeMoco into an EPR silent, integer spin state (M^R), likely $S = 2$. The resultant oxidized Av2 ($Av2^{Ox}$) is diamagnetic. Therefore, the initial one-electron transfer step results in both Av1 and Av2 becoming EPR silent.

Following electron transfer, the two proteins separate in a series of events that involve ATP hydrolysis. The resultant oxidized $Av2^{Ox}(MgADP)_2$ exchanges ADP for ATP and is again reduced, allowing it to undergo another electron transfer cycle [called the Lowe−Thorneley (LT) Fe protein cycle[1]]. According to the generally accepted overall reaction for dinitrogen reduction

$$N_2 + 8e^- + 8H^+ + 16ATP \rightarrow 2NH_3 + H_2 + 16ADP + 16P_i \quad (I)$$

eight one-electron transfer cycles are needed for each molecule of N_2 reduced.

CO is a potent inhibitor of nitrogenase activity except for dihydrogen evolution. When added to a turnover mixture, CO generates different EPR signals. One signal (lo-CO, g [2.09, 1.97, 1.93]) occurs at low CO partial pressures (0.08 atm).[6] This signal is displaced by a second signal (hi-CO, g [2.17, 2.06, 2.06]) as the CO partial pressure is increased (0.5 atm). Both signals require active turnover to be generated. It has previously been shown[7] that rapid EG quenching of a nitrogenase turnover mixture in the presence of high partial pressures of CO stabilizes hi-CO, even though active turnover had ceased. Evacuation of CO from the headspace over the sample induced a conversion of hi-CO to lo-CO, while a subsequent increase in CO partial pressure reverted the system back to hi-CO, again in the absence of active turnover. The hi-CO and/or lo-CO signals persisted as long as CO was present in the headspace.

Much of the nitrogenase mechanism has been studied by ENDOR spectroscopy, while reaction kinetic studies have

Received: April 20, 2015
Revised: June 16, 2015
Published: June 19, 2015

DOI: 10.1021/acs.biochem.5b00426
Biochemistry 2015, 54, 4208−4215

utilized stopped-flow (SF) and freeze-quench (FQ) techniques.[8−13] ENDOR spectroscopy has revealed electronic and binding properties of the different reaction intermediate states.[14] SF has been used to investigate the kinetics and mechanism of the initial electron transfer reaction, while FQ has been mainly utilized in conjunction with EPR and Mössbauer spectroscopies to monitor the generation of different reaction intermediates. This work describes the use of EG to rapidly quench the nitrogenase reaction at room temperature. There are several advantages to using this technique. Unlike FQ, EG can quench enzymatic reactions at room temperature, thus allowing the optical monitoring of intermediates and subsequent relaxation processes under ambient conditions. Also, because EG forms an optical glass of frozen aqueous systems, absorption monitoring techniques, such as MCD and XAS spectroscopies, incompatible with FQ, can be used to characterize reaction intermediates.

As discussed above, nitrogenase exists as a mixture of various reduced states during enzymatic turnover. EG was used to quickly stop nitrogenase turnover, and EPR spectroscopy was subsequently used to monitor the relaxation of the various reduction states back to their resting state. Using this quenching technique, the mechanism of CO binding was also investigated.

MATERIALS AND METHODS

Unless noted otherwise, all chemicals and reagents were obtained from Fisher Scientific or Sigma-Aldrich.

Cell Growth and Protein Purification. *A. vinelandii* strain UW was used to isolate the wild-type Mo-nitrogenase, while *A. vinelandii* strain LS15 was used for the isolation of V-nitrogenase.[3,15] All strains were grown in 180 L batches in a 200 L New Brunswick fermentor in Burke's minimal medium (containing 40 μM V_2O_5 when LS15 was grown to induce the expression of the V-nitrogenase) supplemented with 2 mM ammonium acetate. The growth rate was monitored by cell density at 436 nm. Upon the consumption of ammonia, the cells were derepressed for 3 h and subsequently harvested using a flow-through centrifuge. The Fe protein, MoFe protein (Av1), and VFe protein ($Av1^V$) used in this work were purified as described previously.[3] All purified proteins were stored in 50 mM Tris-HCl (pH 8.0) buffer containing 2 mM sodium dithionite (DTN).

Specific Activity Determination. Acetylene reduction was used monitor protein activity.[3] Samples of component 1 were titrated with component 2 [specific activity of 1800 nmol of ethylene produced min^{-1} (mg of protein)$^{-1}$] to determine the maximal specific activity. A gas chromatograph (Schmadzu, model GC-8A) fitted with a Porapac N column was used to measure ethylene generation. The protein concentration was determined by the biuret method using bovine serum albumin as a protein standard. The specific activity of $Av1^V$ is 245 nmol of C_2H_2 reduced min^{-1} (mg of protein)$^{-1}$, while that of Av1 is 1840 nmol of C_2H_2 reduced min^{-1} (mg of protein)$^{-1}$ consistent with previous purifications.[3]

EPR Spectroscopy. EPR spectra were recorded at cryogenic temperatures (8−12 K, 10 mW) on a Bruker ER 300D spectrometer interfaced to a Bruker 1600 computer for data storage and manipulations. An Oxford Instrument ER-900 helium-flow cryostat positioned in a TE_{102} cavity was used to reach low temperatures. The temperature was monitored and controlled by using an Oxford Instrument model ITC4 temperature controller with a digital readout.

Preparation of EG-Quenched Samples. A nitrogenase turnover sample containing Av1 (10 μM) and Av2 (40 μM or [Av2]:[Av1] = 4) was prepared. An ethylene glycol solution (80% v/v with 2 mM DTN) was rapidly added to the turnover solution (final EG concentration of 45%) and the solution made homogeneous on a Vortex mixer for 1−2 s. Aliquots were periodically extracted, transferred to EPR tubes, and rapidly frozen in liquid N_2 for future analysis.

In the experiments conducted to investigate the generation of the CO-induced EPR signal, hi-CO, the quenched turnover solution was divided among several stoppered vials. CO was injected (final P_{CO} of 0.5 atm) into each vial at different times following EG quenching and then transferred to EPR tubes and frozen in liquid N_2. All preparations were conducted in an inert atmosphere box (<2 ppm O_2).

RESULTS

Activity Inhibition. Water-soluble components, both inorganic and organic, often interfere with aqueous enzyme activity. The inhibitory effect of EG [as well as glycerol (Gyl) and ethanol (Et)] on nitrogenase activity was tested. As previously shown for salt inhibition,[16] organic inhibition was found to be substrate-independent and inhibited all nitrogenase substrate reductions (i.e., H^+, C_2H_2, and N_2) to the same extent. Figure 1 depicts EG inhibition of C_2H_2 reduction activity by Mo-nitrogenase. The sigmoidal profile is not unique to EG but was also observed when either Gly or Et was used. In fact, a sigmoidal profile is a general characteristic of organic and inorganic inhibition of most common enzymes.[17]

Because the sigmoidal inhibition is a common pattern, the potency of an inhibitor has often been expressed as C_{50}, the

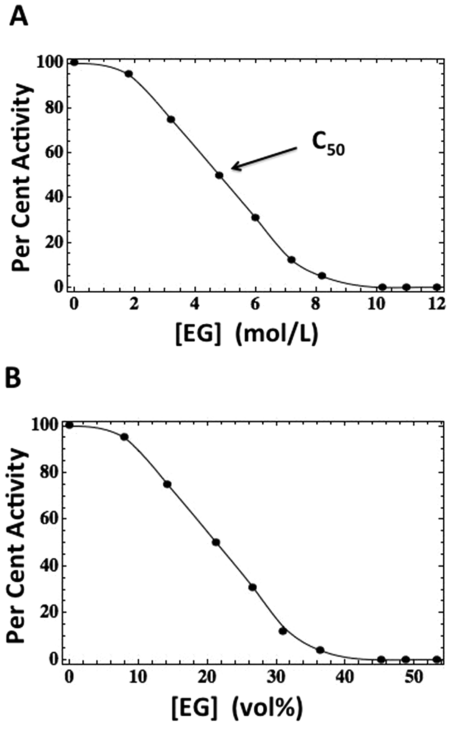

Figure 1. Relative activity of Mo-nitrogenase vs ethylene glycol (EG) expressed in terms of both concentration (A, moles per liter) and volume percent [B, (volume of EG/total volume) × 100]. The solid lines do not represent any equation but only an interpolation of the data to aid the eye.

DOI: 10.1021/acs.biochem.5b00426
Biochemistry 2015, 54, 4208−4215

concentration corresponding to 50% inhibition (Figure 1). Table T1 of the Supporting Information lists C_{50} values (moles per liter) for EG, Gly, and Et inhibition of various enzymes. This table contains several interesting patterns. First, the relative magnitude of C_{50} among the three cosolvents exhibits the same trend for all the enzymes (e.g., Gly is approximately half as potent while EG approximately one-third as potent as Et for each enzyme). Second, the C_{50} values of laccase, α-chymotrypsin, and trypsin are approximately the same for each organic and represent the typical magnitude observed for most common enzymes. By comparison, the C_{50} values for these enzymes are approximately 3 times greater than those of Mo-nitrogenase.

EG easily and rapidly mixes with aqueous solutions and is one of the most common aqueous cryoprotectants. Because of this, it is important to determine the mechanism of EG inhibition of Mo-nitrogenase activity and will be the focus of the rest of this work.

Effect of EG on the Av2:Av1 Ratio for Maximal Activity. The proper way to determine specific activity of the MoFe protein is to titrate it with the Fe protein until maximal activity is achieved. This Av2:Av1 ratio is typically around 8 in normal buffer. To determine whether EG affects this ratio, the maximal activity of Av1 was determined for different EG concentrations (Figure 2). This figure shows that as the EG concentration increases, the Av2:Av1 ratio required for maximal activity also increases.

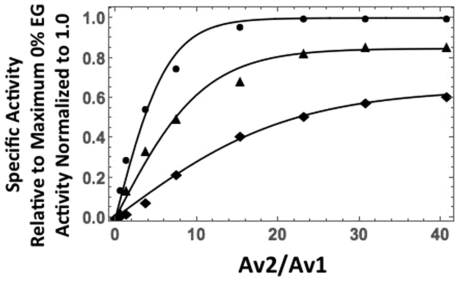

Figure 2. Activity of Mo-nitrogenase vs [Av2]/[Av1] for 0% (●), 12% (▲), and 18% (◆) EG. Activities shown are normalized to the maximal activity of 0% EG = 1.0. The solid lines do not represent any equation but only an interpolation of the data to aid the eye.

Effect of Limiting ATP. For enzymatic turnover, two ATP molecules (as MgATP) must be bound to the Fe protein prior to formation of the Av2−Av1 enzyme complex. Between the events of enzyme complex formation and dissociation, ATP hydrolysis and electron transfer occur (Figure 3). The

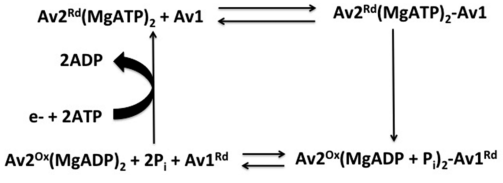

Figure 3. Flowchart of the Lowe−Thorneley Fe protein cycle of Mo-nitrogenase. The cycle begins when $Av2^{Red}(2MgATP)_2$ binds to Av1. This is followed by an electron transfer and ATP hydrolysis to produce $Av2^{Ox}(2MgADP)_2$ and $Av1^{Red}$. $Av2^{Ox}(2MgADP)_2$ then dissociates, replaces ATP for ADP, is reduced to form $Av2^{Red}(2MgATP)_2$, and starts the cycle again.

sequential ordering of ATP hydrolysis and electron transfer is still uncertain; however, recently published data suggest that electron transfer precedes ATP hydrolysis. What is known is that ATP hydrolysis is absolutely necessary for "normal" (i.e., *in vivo*) enzyme activity. Enzyme activity, however, has recently been demonstrated in the absence of ATP hydrolysis with certain protein variants and constructs.[18−20]

Duplicate turnover samples containing limiting ATP were prepared. One sample was in normal buffer, while the two others contained 14 and 20% EG, levels that partially inhibit activity. Acetylene reduction was monitored every 3−5 min until activity ceased because of the depletion of ATP (Figure 4). Upon depletion, all three samples generated the same

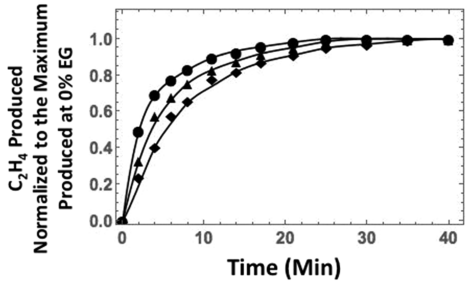

Figure 4. C_2H_4 generated by Mo-nitrogenase under the conditions of limiting ATP. Values for 0% (●), 14% (▲), and 20% (◆) EG are plotted. Note that even though the 14 and 20% EG plots generate C_2H_4 at a slower rate, the final amount produced is the same in plots, meaning the EG does not uncouple ATP hydrolysis from product formation. Plots at 14 and 20% EG are relative to the 0% plot where the maximal level of product produced has been normalized to 1.0. The solid lines do not represent any equation but only an interpolation of the data to aid the eye.

quantity of ethylene even though the samples containing EG took longer to do this. This means that ATP hydrolysis remains coupled to substrate reduction in the presence of EG.

Relaxation of Nitrogenase Intermediate States following EG Quenching. Concentrations of EG above 40% completely inhibit nitrogenase activity (Figure 1). EG (final concentration of 45%) was rapidly mixed (see Materials and Methods) with a nitrogenase turnover mixture, after which activity was periodically measured. The shortest monitoring time (~7 s) demonstrated the complete cessation of activity (Figure 5).

EPR spectroscopy was used in a similar experiment to follow the time course of the Av1 and Av2 intermediate states following EG quenching. A moderate-to-high flux sample (4:1

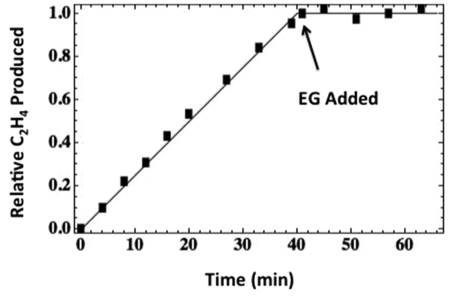

Figure 5. Generation of C_2H_4 followed by rapid EG quenching at 40 min. The reaction utilized an ATP regenerating solution. Note that the C_2H_4 generation immediately ceases upon EG quenching.

DOI: 10.1021/acs.biochem.5b00426
Biochemistry 2015, 54, 4208−4215

Av2:Av1) was allowed to undergo enzymatic turnover. Consistent with similar past studies,[21] the magnitude of the M^N signal decreased within 3 min to a steady state value of ~8% of its as-isolated amplitude. During the same time period, the intensity of the $Av2^{Rd}$ signal decreased by a similar amount. At this point, turnover was rapidly quenched with EG (final concentration of 45%) and EPR samples were periodically extracted, rapidly frozen, and subsequently analyzed (Figures 6

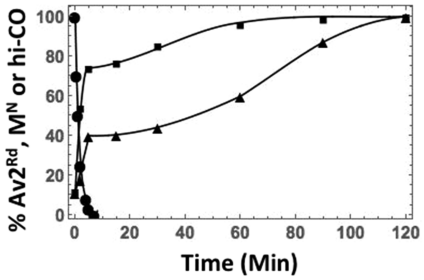

Figure 6. Relative intensity [measured from the EPR spectra (see Figure 7)] of the $S = {}^1/_2$ state of $Av2^{Rd}$ (■) and the $S = {}^3/_2$ state of M^N (▲) of FeMoco following EG quenching. Also shown is the relative intensity of the hi-CO EPR signal (●) generated when CO was added after EG quenching. The solid lines do not represent any equation but only an interpolation of the data to aid the eye.

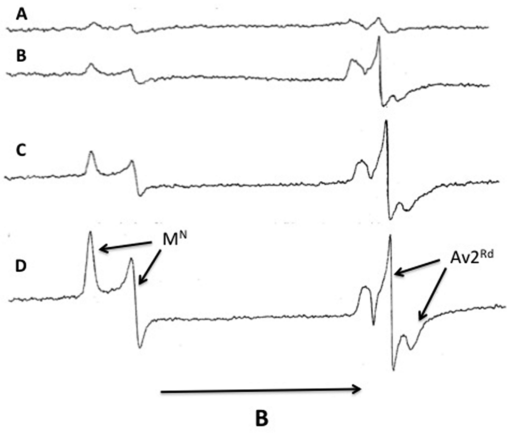

Figure 7. EPR spectra of the turnover mixture: (A) frozen during turnover (0% EG) × 4, (B) frozen 2 min after EG quenching, (C) frozen 5 min after EG quenching, and (D) frozen 120 min after EG quenching. Spectral parameters: modulation amplitude, 0.3 mT; microwave frequency, 9.45 GHz; temperature, 7 K; microwave power, 10 mW.

and 7). Both M^N and $Av2^{Rd}$ recovered to their resting concentrations in two phases, one rapid and one slow. In the first (rapid) phase (0–5 min), $Av2^{Rd}$ returned to ~74% of its normal intensity while M^N returned to ~50% of its normal intensity. In the second (slow) phase (5–120 min), both $Av2^{Rd}$ and M^N signal recoveries exhibited sigmoidal characteristics.

Effect of Adding CO after EG Quenching. The ability of a nitrogenase turnover mixture to generate the hi-CO signal following EG quenching was tested (Figure 8). Adding CO (0.5 atm) to the reaction headspace just prior to EG quenching resulted in a fully developed hi-CO signal. Reversing the order [i.e., adding CO immediately (<5 s) after EG quenching] resulted in the generation of both lo-CO and hi-CO. Addition

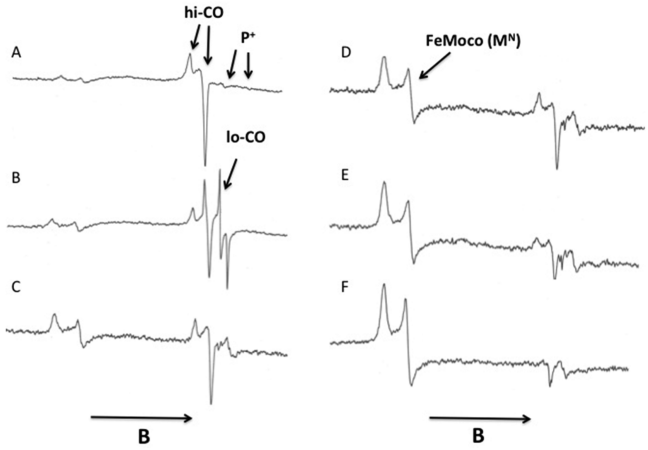

Figure 8. Effect of adding CO (0.5 atm) on the EPR spectra of a turnover mixture before and after EG quenching: (A) CO added before EG quenching, (B) CO added immediately after EG quenching, (C) CO added 20 s after quenching, (D) CO added 1 min after quenching, (E) CO added 4 min after quenching, and (F) CO added 5 min after quenching. Spectral parameters: modulation amplitude, 0.3 mT; microwave frequency, 9.46 GHz; temperature, 10 K; microwave power, 10 mW.

of CO at later times following EG quenching resulted in the generation of only hi-CO whose amplitude decreased with increasing time. This process continued until 5 min, after which no CO signal was detected upon the addition of CO even though a significant percentage of Av1 was still in the EPR silent M^R state.

DISCUSSION

Organic Cosolvent Quenching of Nitrogenase Activity. Sigmoidal inhibition of enzyme activity (Figure 1) typically implies cooperativity. A Hill plot of the Et, Gly, and EG inhibition of Mo-nitrogenase (Figure S1 of the Supporting Information) yields a cooperativity factor of 2 for all three cosolvents. This suggests that there are two inhibition sites on nitrogenase. As will be discussed below, inhibition is likely the organic solvent interfering with the binding of two ATP molecules to the Fe protein, consistent with the Hill plot.

Unlike other enzymes (Table T1 of the Supporting Information), organic inhibition of nitrogenase occurs at much lower concentrations. Organic inhibition is often associated with enzyme denaturation, as suggested by changes in the enzyme's spectroscopic properties. This is not the case for Mo-nitrogenase where no changes in the EPR spectrum of Av1 were detected over the entire range of inhibition concentrations. Furthermore, EG inhibition of Mo-nitrogenase is completely reversible, suggesting that it is not due to degradation.

Nitrogenase activity requires the concerted interactions of Av1, Av2, and MgATP. As such, inhibition may be a result of cosolvent binding to and/or interfering with one or more of these components. The rate-limiting step of the nitrogenase catalytic cycle is the dissociation of $Av2^{Ox}(MgADP)_2$ from Av1 following ATP hydrolysis and electron transfer.[22] Organic solvents have been shown[13] to retard the rate of transfer of an electron from Av2 to Av1 and may similarly retard dissociation of the two proteins. However, the studies presented here demonstrate that the Av2:Av1 component ratio needed for maximal activity (Figure 2) increases with an increasing EG

DOI: 10.1021/acs.biochem.5b00426
Biochemistry 2015, 54, 4208–4215

concentration, a relationship that would not occur if EG only retarded protein dissociation.

The nitrogenase mechanism is traditionally described by the Lowe−Thorneley (LT) MoFe protein cycle.[1] This cycle involves the transfer of eight electrons for complete N_2 fixation (Figure 3). In the absence of an external substrate, only H_2 evolution occurs and the LT cycle is truncated such that a maximum of four electrons is transferred (Figure 9). In this

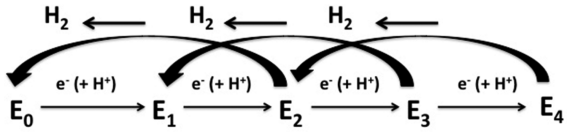

Figure 9. Truncated Lowe−Thorneley nitrogenase turnover cycle. State $\mathbf{E}_n$ represents one-half of the MoFe protein (containing one FeMoco) following the transfer of n electrons (right-pointing arrows) from the Fe protein (along with n protons). Relaxation (left-pointing arrows) occurs when a reduced state ($n \geq 2$) emits H_2 and drops to a lower $\mathbf{E}_n$ state ($\mathbf{E}_n \rightarrow \mathbf{E}_{n-2} + H_2$).

cycle, the reduction state of each $\alpha\beta$ half of the MoFe protein (containing one FeMoco and one P-cluster) is designated as $\mathbf{E}_n$, where n equals the number of electrons (and protons) transferred. In this notation, the resting state is $\mathbf{E}_0$, the state after one electron transfer is $\mathbf{E}_1$, etc. After the system has accumulated at least two electrons ($\mathbf{E}_n$, where $n \geq 2$), it will either be further reduced to the next state ($\mathbf{E}_{n+1}$) or it will relax to state $\mathbf{E}_{n-2}$ with the evolution of H_2. Under low-flux conditions (a low Av2:Av1 ratio), the rate of relaxation ($\mathbf{E}_2 \rightarrow \mathbf{E}_0$) is faster than the rate of reduction ($\mathbf{E}_2 \rightarrow \mathbf{E}_3$) and the steady state exists as approximately equal amounts of $\mathbf{E}_0$ and $\mathbf{E}_1$ with a small amount of $\mathbf{E}_2$. Under moderate- to high-flux conditions in the absence of an external substrate, the rate of reduction exceeds the rate of relaxation and more reduced states of $\mathbf{E}_2$, $\mathbf{E}_3$, and $\mathbf{E}_4$ (Figure 9) exist in the steady state. Past studies suggest that states $\mathbf{E}_2$−$\mathbf{E}_4$ are associated with substrate binding and reduction.[1] The proposed binding at the $\mathbf{E}_2$−$\mathbf{E}_4$ states has been characterized by ENDOR spectroscopy.[23−25]

EG quenching of a nitrogenase activity reveals several interesting facts about the enzymatic mechanism (Figures 7 and 10) not previously observed with other techniques. During the 5 min interval following quenching, the EPR signals of both M^N and $Av2^{Rd}$ rapidly recover to part of their original resting state intensities. Past studies[1] show that the rapid recovery of $Av2^{Rd}$

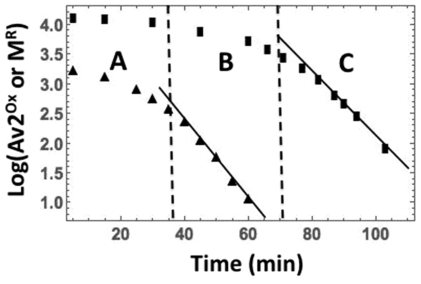

Figure 10. Semilog plot of the decay of $Av2^{Ox}$ (▲) and M^R (■). Region A represents the time period during which neither species exhibits a significant decay. In region B, $Av2^{Ox}$ exhibits a slow first-order decay followed by a subsequent slow first-order decay of M^R in region C.

is due to the reduction of free $Av2^{Ox}$ by DTN (k = 646 s^{-1} in buffer).

The rapid recovery phase of M^N, on the other hand, is most likely due to the relaxation of more reduced states [i.e., $\mathbf{E}_n \rightarrow \mathbf{E}_{n-2} + H_2$ (see Figure 10)]. Specifically, reduced states with n being an even number ($\mathbf{E}_4$ and $\mathbf{E}_2$) will eventually relax to $\mathbf{E}_0$ (yielding EPR active M^N), while the $\mathbf{E}_3$ state will relax to $\mathbf{E}_1$ (with EPR silent M^R) as described by the LT cycle (note that the rate of relaxation in the presence of 45% EG may differ from the rates observed in aqueous buffer) and shown in quench-cryoannealing studies.[23] The rapid recovery of 50% of the as-isolated Av1 implies that, during active turnover, approximately half of the $\mathbf{E}_n$ states are integer spin states (n being an odd number) while the other half are half-integer states (n being an even number). According to the LT cycle, all relaxations occur in steps of 2 ($\mathbf{E}_n \rightarrow \mathbf{E}_{n-2} + H_2$), meaning $\mathbf{E}_1$ cannot relax to $\mathbf{E}_0$. It will be shown below that this assumption is not correct in our system.

Following the initial fast recovery of the EPR active states, the profiles of the slow recovery of the remaining $Av2^{Rd}$ and M^N are unexpected (Figure 6). Both slow recoveries exhibit sigmoidal characteristics, implying more than one mechanistic step (labeled regions A−C in Figure 10). As mentioned above, free $Av2^{Ox}$ is rapidly reduced by DTN (eq I). This suggests that the long-lived form of $Av2^{Ox}$ is not free but is still bound to Av1 and, as such, is not readily accessible to DTN reduction. As will be argued below, the long-lived $Av2^{Ox}$ is most likely bound to the Av1 half that is still in the EPR silent $\mathbf{E}_1$ state, i.e., ($Av2^{Ox}$-$\mathbf{E}_1$). After the initial 5 min rapid relaxation of $Av2^{Ox}$ and prior to the slow recovery phase (region B), there is a lag period (region A) during which little $Av2^{Ox}$ or $\mathbf{E}_1$ relaxes to its native state. This lag is likely associated with one or more structural changes in the ($Av2^{Ox}$-$\mathbf{E}_1$) complex, eventually converting it to a form, ($Av2^{Ox}$-$\mathbf{E}_1$)*, in which $Av2^{Ox}$ is more susceptible to DTN reduction to $Av2^{Rd}$. In other words, in region A

$$(Av2^{Ox}\text{-}\mathbf{E}_1) \xrightarrow{slow} (Av2^{Ox}\text{-}\mathbf{E}_1)^* \quad (1)$$

followed by (in region B)

$$(Av2^{Ox}\text{-}\mathbf{E}_1)^* \xrightarrow{DTN,slow} (Av2^{Rd}\text{-}\mathbf{E}_1)^* \xrightarrow{fast} Av2^{Rd} + \mathbf{E}_1 \quad (2a)$$

and/or

$$(Av2^{Ox}\text{-}\mathbf{E}_1)^* \xrightarrow{slow} Av2^{Ox} + \mathbf{E}_1 \xrightarrow{DTN,fast} Av2^{Rd} + \mathbf{E}_1 \quad (2b)$$

The identity of the structural change(s) in region A (eq I) is unknown. It may involve a slow conformational and/or structural rearrangement of the $Av2^{Ox}$-$\mathbf{E}_1$ complex. X-ray diffraction techniques have revealed several different structural docking arrangements of the Av2-Av1 complex.[26] ($Av2^{Ox}$-$\mathbf{E}_1$) and ($Av2^{Ox}$-$\mathbf{E}_1$)* may correspond to one or more of these structures.

A semistable ($Av2^{Ox}$-$\mathbf{E}_1$) complex, as suggested by the data here, has not been previously reported for *A. vinelandii* nitrogenase. Other tight-binding, inactive nitrogenase complexes have been described in the past. For example, the Fe protein from *Clostridium pasteurianum* forms a tight-binding complex when mixed with Av1 and MgATP.[27] The dissociation of this complex is slower (k = 0.35 s^{-1}) than that of the homologous Av2-Av1 couple (k = 7 s^{-1}). A tight-binding complex is also formed between the variant L127Δ Av2 and Av1. L127Δ Av2 possesses that unusual property of exhibiting spectral properties normally observed upon ATP binding.[28]

DOI: 10.1021/acs.biochem.5b00426
Biochemistry 2015, 54, 4208−4215

L127Δ Av2 forms a tight-binding complex with Av1 in the absence of ATP. However, because there is no ATP bound, this complex does not support substrate reduction and exhibits a very slow dissociation (k = 0.02 s^{-1}).

The $Av2^{Ox}$-$\mathbf{E_1}$ complex proposed here appears to have been formed as a result of the rapid EG quenching. Because EG likely interferes with ATP binding (see below), the stability of this complex in EG may be due to the absence of bound ATP. In other words, the stability of this complex suggests that ATP binding and/or hydrolysis is a necessary part of dissociation of the Av2-Av1 complex.

A semilog plot (Figure 10) of the recovery of $Av2^{Rd}$ (eq 2a and/or 2b) exhibits first-order kinetics [k_{Fe} = (1.1 ± 0.5) × 10^{-3} s^{-1}] in region B. Two possible mechanisms for this recovery are proposed in eq 2. In eq 2a, the rate-limiting step is the slow penetration of DTN into the $[Fe_4S_4]^{2+}$ site in ($Av2^{Ox}$-$\mathbf{E_1}$)*. In eq 2b, the rate-limiting step is the slow dissociation of ($Av2^{Ox}$-$\mathbf{E_1}$)* into $Av2^{Ox}$ + $\mathbf{E_1}$, after which free $Av2^{Ox}$ is rapidly reduced by DTN.

It is well established that the shape of the EPR spectrum of $Av2^{Rd}$ changes upon MgATP binding. In the absence of ATP, the spectrum is rhombic (g factors of 2.06, 1.94, and 1.86) and shifting to axial (g factors of 2.04, 1.90, and 1.90) upon MgATP binding. Even though ATP is present in our turnover mixture, the $Av2^{Rd}$ EPR signal, after EG quenching, exhibits the rhombic shape (Figure 7) more associated with ATP free $Av2^{Rd}$. This is not unexpected, and the effect of EG on the Fe protein EPR spectrum in the presence of ATP has previously been observed.[29−31] Furthermore, MCD spectroscopy has illustrated that both free $Av2^{Rd}$ and $Av2^{Rd}$ + Mg + ATP exhibit essentially identical electronic structures and spin state mixtures when EG is present, suggesting that EG inhibits binding of MgATP to Av2.[32]

It is generally agreed that ATP generates a structure and/or redox potential in $Av2^{Rd}$ necessary for catalytic activity. The model presented here is that EG inhibition is due, at least in part, to its blocking of binding of ATP to $Av2^{Rd}$, thus preventing it from achieving the proper structural form for binding and productive ET. In this model, $Av2^{Rd}$ would exist as $Av2^{Rd}(MgATP)_2$ (100% activity) in buffer and as free $Av2^{Rd}$ (0% activity) in ≥40% EG. For EG concentrations between 0 and 40%, the solution likely contains a mixture of these two forms and possibly some $Av2^{Rd}$(MgATP). This model correctly predicts that EG does not uncouple ATP hydrolysis from substrate reduction (Figure 4); it simply reduces that relative concentration of the catalytically active form of the Fe protein, $Av2^{Rd}(MgATP)_2$. In the presence of EG, the total concentration of Av2 must increase (Figure 2) to achieve the necessary concentration of $Av2^{Rd}(MgATP)_2$ for maximal Av1 activity. This means that as the EG concentration increases, the Av2:Av1 ratio required for maximal activity also increases (Figure 2).

The slow phase recovery of the EPR spectrum of M^N, following EG quenching of activity, exhibits sigmoidal properties similar to those of the recovery of $Av2^{Rd}$. In our model, this recovery traces the relaxation of $\mathbf{E_1}$ (M^R) to $\mathbf{E_0}$ (M^N) and occurs after the conversion of $Av2^{Ox}$ to $Av2^{Rd}$ (region B), suggesting that the two reactions are consecutively linked. This will happen if $Av2^{Ox}$ is bound to the side of Av1 that is in the $\mathbf{E_1}$ state, i.e., ($Av2^{Ox}$-$\mathbf{E_1}$). As $Av2^{Ox}$ is reduced, the $\mathbf{E_1}$ state is free (eq 2) to relax to the $\mathbf{E_0}$ state.

As with ($Av2^{Ox}$-$\mathbf{E_1}$)*, the relaxation of $\mathbf{E_1}$ to $\mathbf{E_0}$ follows pseudo-first-order kinetics (region C in Figure 10) with a rate constant [k_M = (0.90 ± 0.06) × 10^{-3} s^{-1}] similar to the rate constant (k_{Fe}) deduced for the relaxation of ($Av2^{Ox}$-$\mathbf{E_1}$)*. Two possible mechanisms for the relaxation of free $\mathbf{E_1}$ are

$$\mathbf{E_1} + \mathbf{E_1} \rightarrow \mathbf{E_2} + \mathbf{E_0} \rightarrow 2\mathbf{E_0} + H_2 \quad (3)$$

and

$$\mathbf{E_1} \rightarrow \mathbf{E_0} \quad (4)$$

Equation 3 can be ruled out because it does not follow first-order kinetics, leaving eq 4 as the most likely mechanism for the relaxation of $\mathbf{E_1}$. Data have been published[23] recently showing that $\mathbf{E_1}$ does not relax to $\mathbf{E_0}$ in the frozen state, were it to be immobilized. This is obviously not the case when $\mathbf{E_1}$ is free in solution.

In an early study, the oxidation of free $\mathbf{E_1}$ to $\mathbf{E_0}$ was monitored.[33] In that study, a *C. pasteurianum* W5Mo-nitrogenase turnover mixture was chromatographed on a short DEAE-cellulose column to rapidly separate the MoFe protein from ATP and the Fe protein. After separation, some of the isolated MoFe protein still exhibited the $\mathbf{E_1}$ state. As in the study described here, the conversion of $\mathbf{E_1}$ to $\mathbf{E_0}$ was monitored by EPR spectroscopy. Unlike the results presented here, this conversion exhibited straight first-order kinetics without any sigmoidal behavior or lag periods (Figure 10, regions A and B). This is consistent with our model in which the sigmoidal behavior or lag periods are associated with the conversion of complexes ($Av2^{Ox}$-$\mathbf{E_1}$) and ($Av2^{Ox}$-$\mathbf{E_1}$)* and the dissociation of the latter. These complexes would not be present in the DEAE study (i.e., there is no *C. pasteurianum* Fe protein present). Of greater significance, the kinetic rate constant of the conversion of $\mathbf{E_1}$ to $\mathbf{E_0}$ measured in the DEAE study [k_{DEAE} = (0.96 ± 0.10) × 10^{-3} s^{-1}] is essentially identical to that observed in this study. This further supports the model in which the $\mathbf{E_1} \rightarrow \mathbf{E_0}$ conversion in the study here involves only the free MoFe protein.

The oxidation of $\mathbf{E_1}$ to $\mathbf{E_0}$ may be aided by DTN. While DTN is a reductant, it has never been shown to reduce $\mathbf{E_0}$ to $\mathbf{E_1}$, and it certainly does not oxidize the cofactor. However, its presence may assist in, or mediate, the oxidation of $\mathbf{E_1}$. At pH 7.4, a DTN solution will contain a mixture of $S_2O_4^{2-}$ and SO_2^- ions

$$S_2O_4^{2-} \leftrightarrow 2SO_2^- \quad (5)$$

as well as the oxidation product, SO_3^{2-}. The slow decay of free $\mathbf{E_1}$ (eq 4) may be aided by the slow penetration of one or more of these ions into the FeMoco (M^R) site in Av1. The fact that the rate constant for the relaxation of $Av2^{Ox}$ to $Av2^{Rd}$ is nearly the same as the rate constant for the conversion of $\mathbf{E_1}$ to $\mathbf{E_0}$ may be coincidental but lends strength to eq 2a being the mode of relaxation of $Av2^{Ox}$.

Generation of hi-CO and lo-CO following EG Quenching. It has always been assumed the CO-induced EPR signals, hi-CO and lo-CO, can be generated only during active turnover. Therefore, it is interesting that these signals are observed immediately following EG quenching even though enzymatic activity has terminated. This suggests that the reactive states, needed for the generation of these signals, are still present for a short time period following EG quenching. During active turnover, lo-CO is observed only under moderate- to high-electron flux conditions, implying that its formation requires a more reduced state such as $\mathbf{E_3}$ or $\mathbf{E_4}$.[7] On the other hand, hi-CO is formed under all flux conditions. In the study presented here, lo-CO is observed only during the

DOI: 10.1021/acs.biochem.5b00426
Biochemistry 2015, 54, 4208−4215

first 5−10 s following EG quenching, a time during which states $\mathbf{E}_3$ and $\mathbf{E}_4$ likely still exist, albeit at low concentrations. On the other hand, hi-CO is generated up to 5 min after EG quenching. Because our model proposes that states $\mathbf{E}_1$ and $\mathbf{E}_0$ dominate after 5 min, hi-CO can likely be generated by state $\mathbf{E}_2$.

CONCLUSIONS

The data presented here illustrate several interesting factors concerning the nitrogenase mechanism. First, the source of EG inhibition is likely the blocking of MgATP binding to Av2. A possible similar inhibition by polyglycols may be the reason why diffracting crystals of ATP bound to the Fe protein have not been obtained to date. Furthermore, EG quenching illustrates that several intermediate turnover states can be stabilized, requiring long time periods for eventual relaxation to the as-isolated state. It also illustrates that there are likely several different structural forms of ($Av2^{Ox}$-$\mathbf{E}_1$). The stability of these structures suggests that ATP hydrolysis is necessary for complex dissociation. Finally, EG quenching allows for a more in-depth investigation of CO binding, showing that turnover mixtures still retain the ability to generate the CO-induced EPR signals, lo-CO and hi-CO, in the absence of turnover.

ASSOCIATED CONTENT

Supporting Information

Hill plots for the inhibition of Mo-nitrogenase by ET, Gly, and ET and a table containing the C_{50} inhibition concentrations for several common globular proteins as well as Mo-nitrogense and V-nitrogenase. The Supporting Information is available free of charge on the ACS Publications website at DOI: 10.1021/acs.biochem.5b00426.

AUTHOR INFORMATION

Corresponding Author

*E-mail: bhales@lsu.edu. Telephone: (225) 578-4694.

Funding

This work is supported by the Louisiana Board of Regents (EPSCoR 2013 Pfund-308).

Notes

The authors declare no competing financial interest.

ABBREVIATIONS

ENDOR, electron nuclear double resonance; Av2, Fe protein of Mo-nitrogenase from *A. vinelandii*; Av1, MoFe protein of Mo-nitrogenase from *A. vinelandii*; $Av1^V$, VFe protein of V-nitrogenase from *A. vinelandii*; FeMoco, FeMo cofactor at the active site on the MoFe protein of nitrogenase; DTN, sodium dithionite; EG, ethylene glycol; Gyl, glycerol; Et, ethanol; FQ, freeze-quench; SF, stopped-flow; MCD, magnetic circular dichroism; C_{50}, concentration of 50% inhibition of activity.

REFERENCES

(1) Burgess, B. K., and Lowe, D. J. (1996) Mechanism of Molybdenum Nitrogenase. *Chem. Rev. 96*, 2983−3011.

(2) Robson, R. L., Eady, R. R., Richardson, T. H., Miller, R. W., Hawkins, M., and Postgate, J. R. (1986) The Alternative Nitrogenase of *Azotobacter chroococcum* is a Vandium Enzyme. *Nature 322*, 388−390.

(3) Hales, B. J., Case, E. E., Morningstar, J. E., Dzeda, M. F., and Mauterer, L. A. (1986) Isolation of a New Vanadium-Containing Nitrogenase from *Azotobacter vinelandii*. *Biochemistry 25*, 7251−7255.

(4) Münck, E., Rhodes, H., Orme-Johnson, W. H., Davis, L. C., Brill, W. J., and Shah, V. K. (1975) The MoFe Protein Component from *Azotobacter vinelandii*. *Biochim. Biophys. Acta 400*, 32−53.

(5) Lindahl, P. A., Day, E. P., Kent, T. A., Orme-Johnson, W. H., and Münck, E. (1985) Mössbauer, EPR, and Magnetization Studies of the *Azotobacter vinelandii* Fe Protein. *J. Biol. Chem. 260*, 11160−11173.

(6) Davis, L. C., Henzl, M. T., Burris, R. H., and Orme-Johnson, W. H. (1979) Iron-Sulfur Clusters in the Molybdenum-Iron Protein Component of Nitrogenase. Electron Paramagnetic Resonance of the Carbon Monoxide Inhibited State. *Biochemistry 18*, 4860−4869.

(7) Cameron, L. M., and Hales, B. J. (1998) Investigation of CO Binding and Release from Mo-Nitrogenase during Catalytic Turnover. *Biochemistry 37*, 9449−9456.

(8) Thorneley, R. N. F. (1975) Nitrogenase of *Klebsiella pneumoniae*: A Stopped-Flow Study of Mg-ATP-Induced Electron Transfer between the Component Proteins. *Biochem. J. 145*, 391−396.

(9) Thorneley, R. N. F., Yates, M. G., and Lowe, D. J. (1976) Nitrogenase of *Azotobacter chroococcum* Kinetics of the Reduction of Oxidized Iron-Protein by Sodium Dithionite. *Biochem. J. 155*, 137−144.

(10) Thorneley, R. N. F., and Lowe, D. J. (1982) Mechanistic Studies on Nitrogenase from *Klebsiella pneumoniae* Using the Rapid Quench Technique. *Isr. J. Bot. 31*, 61−71.

(11) Thorneley, R. N. F., Deistung, J., Cannon, F. C., Cannon, M. C., and Hill, S. (1985) Electron Transfer to Nitrogenase in *Klebsiella pneumoniae*. *Biochem. J. 231*, 743−753.

(12) Ryle, M. J., Lee, H.-I., Seefeldt, L. C., and Hoffman, B. M. (2000) Nitrogenase Reduction of Carbon Disulfide: Freeze-Quench EPR and ENDOR Evidence for Three Sequential Intermediates with Cluster-Bound Carbon Moieties. *Biochemistry 39*, 1114−1119.

(13) Danyal, K., Dean, D. R., Hoffman, B. M., and Seefeldt, L. C. (2011) Electron Transfer within Nitrogenase: Evidence for a Deficit-Spending Mechanism. *Biochemistry 50*, 9255−9263.

(14) Cutsail, G. E., III, Telser, J., and Hoffman, B. M. (2015) Advanced Paramagnetic Resonance Spectroscopies of Iron-Sulfur Proteins: Electron Nuclear Double Resonance (ENDOR) and Elecron Spin Echo Envelope Modulation (ESEEM). *Biochim. Biophys. Acta 1853*, 1370−1394.

(15) Hales, B. J., Case, E., and Langosch, D. (1985) Nitrogen Fixation in *nifHDK* Deletion Strains of *Azotobacter vinelandii*. In *Nitrogen Fixation Research Progress* (Evans, H. J., Bottomley, P. J., and Newton, W. E., Eds.) p 612, Martinus Nijhoff Publishers, Dordrecht, The Netherlands.

(16) Deits, T. L., and Howard, J. B. (1990) Effect of Salts on *Azotobacter vinelandii* Nitrogenase Activities. *J. Biol. Chem. 265*, 3859−3867.

(17) Khmelnitsky, Y. L., Mozhaev, V. V., Belova, A. B., Sergeeva, M. V., and Martinek, K. (1991) Denaturation capacity: A new quantitative criterion for selection of organic solvents as reaction media in biocatalysis. *Eur. J. Biochem. 198*, 31−41.

(18) Roth, L. E., Nauven, J. C., and Tezcan, F. A. (2010) ATP- and Iron-Protein-Independent Activation of Nitrogenase Catalysis by Light. *J. Am. Chem. Soc. 132*, 13672−13674.

(19) Roth, L. E., and Tezcan, F. A. (2012) ATP-Uncoupled, SIx-Electron Photoreduction of Hydrogen Cyanide to Methane by the Molybdenum-Iron Protein. *J. Am. Chem. Soc. 134*, 8416−8419.

(20) Danyal, K., Rasmussen, A. J., Keable, S. M., Inglet, B. S., Shaw, S., Zadvornyy, O. A., Duval, S., Dean, D. R., Raugei, S., Peters, J. W., and Seefeldt, L. C. (2015) Fe Protein-Independent Substrate Reduction by Nitrogenase MoFe Protein Variants. *Biochemsitry 54*, 2456−2462.

(21) Hageman, R. V., and Burris, R. H. (1978) Nitrogenase and Nitrogenase Reductase Associate and Dissociate with each Catalytic Cycle. *Proc. Natl. Acad. Sci. U.S.A. 75*, 2699−2702.

(22) Thorneley, R. N. F., and Lowe, D. J. (1983) Nitrogenase of *Klebsiella pneumoniae*. Kinetics of the Dissociation of Oxidized Iron Protein from Molybdenum-iron Protein: Identification of the Rate-limiting Step for Substrate Reduction. *Biochem. J. 215*, 393−403.

DOI: 10.1021/acs.biochem.5b00426
Biochemistry 2015, 54, 4208−4215

(23) Lukoyanov, D., Yang, Z.-Y., Duval, S., Danyal, K., Dean, D. R., Seefeldt, L., and Hoffman, B. M. (2014) A Confirmation of the Quench-Cryoannealing Relaxation Protocol for Identifying Reduction States of Freeze-Trapped Nitrogenase Intermediates. *Inorg. Chem. 53*, 3688−3693.
(24) Shaw, S., Lukoyanov, D., Danyal, K., Dean, D. R., Hoffman, B. M., and Seefeldt, L. C. (2014) Nitrite and Hydroxylamine as Nitrogenase Substrates: Mechanistic Implications for the Pathway of N_2. *J. Am. Chem. Soc. 136*, 12776−12783.
(25) Lukoyanov, D., Yang, Z.-Y., Khadka, N., Dean, D. R., Seefeldt, L. C., and Hoffman, B. M. (2015) Identification of a Key Catalytic Intermediate Demonstrates that Nitrogenase is Activated by the Reversible Exchange of N_2 for H_2. *J. Am. Chem. Soc. 137*, 3610−3615.
(26) Tezcan, F. A., Kaiser, J. T., Mustafi, D., Walton, M. Y., Howard, J. B., and Rees, D. C. (2005) Nitrogenase Complexes: Multiple Docking Sites for a Nucleotide Switch Protein. *Science 309*, 1377−1380.
(27) Emerich, D. W., Ljones, T., and Burris, R. H. (1978) Nitrogenase: Properties of the Catalytically Inactive Complex between the *Azotobacter vinelandii* MoFe Protein and the *Clostridium pasteurianum* Fe Protein. *Biochim. Biophys. Acta 527*, 359−369.
(28) Lanzilotta, W. N., Fisher, K., and Seefeldt, L. C. (1996) Evidence for Electron Transfer from the Nitrogenase Iron Protein to the Molybdenum-Iron Protein without MgATP Hydrolysis: Characterization of a Tight Protein-Protein Complex. *Biochemistry 35*, 7188−7196.
(29) Morgan, T. V., Prince, R. C., and Mortenson, L. E. (1986) Electrochemical Titration of the $S = 3/2$ and $S = 1/2$ States of the Iron Protein of Nitrogenase. *FEBS Lett. 206*, 4−8.
(30) Lindahl, P. A., Gorelick, N. J., Münck, E., and Orme-Johnson, W. H. (1987) EPR and Mössbauer Studies of Nucleotide-Bound Nitrogenase Iron Protein from *Azotobacter vinelandii*. *J. Biol. Chem. 262*, 14945−14953.
(31) Hagen, W. R., Eady, R. R., Dunham, W. R., and Haaker, H. (1985) A Novel $S = 3/2$ EPR Signal Associated with Native Fe-Proteins of Nitrogenase. *FEBS Lett. 189*, 250−254.
(32) Onate, Y. A., Finnegan, M. G., Hales, B. J., and Johnson, M. K. (1993) Variable Temperature Magnetic Circular Dichroism Studies of Reduced Nitrogenase Iron Proteins and $[4Fe\text{-}4S]^+$ Synthetic Analog Clusters. *Biochim. Biophys. Acta 1164*, 113−123.
(33) Orme-Johnson, W. H., Paul, L., Meade, J., Warren, W., Nelson, M., Groh, S., Orme-Johnson, N. R., Münck, E., Huynh, B. N., Emptage, M., Rawlings, J., Smith, J., Roberts, J., Hoffmann, B., and Mims, W. B. (1981) Nitrogenase: Prosthetic Groups and Their Reactivities. In *Current Perspectives in Nitrogen Fixation* (Gibson, A. H., and Newton, W. E., Eds.) pp 79−84, Elsevier, North-Holland, NY.

DOI: 10.1021/acs.biochem.5b00426
Biochemistry 2015, 54, 4208−4215